1   **THYROID STATUS MODULATES T LYMPHOMA GROWTH VIA CELL**

2   **CYCLE REGULATORY PROTEINS AND ANGIOGENESIS**

3   Sterle HA[1], Valli E[1], Cayrol F[1], Paulazo MA[2], Martinel Lamas DJ[3], Diaz Flaqué MC[1],

4   Klecha AJ[3], Colombo L[4], Medina VA[3], Cremaschi GA[1,3], Barreiro Arcos ML[1,5].

5

6   [1]Instituto de Investigaciones Biomédicas (BIOMED), Consejo Nacional de

7   Investigaciones Científicas y Técnicas (CONICET), Facultad de Ciencias Médicas,

8   Pontificia Universidad Católica Argentina (UCA), Buenos Aires, Argentina

9   [2]Centro de Estudios Farmacológicos y Botánicos (CEFYBO), CONICET, Facultad de

10   Medicina, Universidad de Buenos Aires (UBA), Buenos Aires, Argentina.

11   [3]Laboratorio de Radioisótopos, Facultad de Farmacia y Bioquímica, UBA.

12   [4]Area de Investigación, Instituto de Oncología "Angel H. Roffo", UBA, CONICET.

13   [5]Departamento de Química Biológica, Facultad de Ciencias Exactas y Naturales, UBA.

14

15   **Running Title:** Thyroid status modulation of tumor growth

16   **Key words:** Thyroid hormones; T lymphoma; Cell cycle; Angiogenesis

17

18   **Corresponding author:** Drs. María Laura Barreiro Arcos and Graciela Cremaschi,

19   Instituto de Investigaciones Biomédicas (BIOMED), CONICET, UCA. Av. A. Moreau

20   de Justo 1600, 3er piso, 1107AFF, Buenos Aires, Argentina. Phone: +5411-4349-0200

21   ext 1236, Fax: +5411-4349-0200 ext 7121. e-mail mlbarreiro@yahoo.com.ar

22

23

24

25

1

26 **ABSTRACT**

27

28 We have shown *in vitro* that thyroid hormones (THs) regulate the balance between

29 proliferation and apoptosis of T lymphoma cells. The effects of THs on tumor

30 development have been studied, but the results are still controversial. Here, we show the

31 modulatory action of thyroid status on the *in vivo* growth of T lymphoma cells. For this

32 purpose, euthyroid, hypothyroid and hyperthyroid mice were inoculated with EL-4 cells

33 to allow the development of solid tumors. Tumors in the hyperthyroid animals exhibited

34 a higher growth rate, as evidenced by the early appearance of palpable solid tumors and

35 the increased tumor volume. These results are consistent with the rate of cell division

36 determined by staining the tumor cells with CFSE. Additionally, the hyperthyroid mice

37 exhibited reduced survival. The hypothyroid mice were not significantly different from

38 the euthyroid controls in these parameters. Additionally, only tumors from the

39 hyperthyroid animals had increased expression levels of PCNA and active caspase 3.

40 Also, the differential expression of cell cycle regulatory proteins was observed. The

41 levels of cyclins D1 and D3 were augmented in the tumors of the hyperthyroid animals,

42 whereas the cell cycle inhibitors p16/INK4A and p27/Kip1 and the tumor suppressor

43 p53 were increased in the hypothyroid mice. Intratumoral and peritumoral

44 vasculogenesis was increased only in the hyperthyroid mice. Therefore, we propose that

45 the thyroid status modulates the *in vivo* growth of EL-4 T lymphoma through of the

46 regulation of cyclin, cyclin-dependent kinase inhibitor, and tumor suppressor gene

47 expression, as well as the stimulation of angiogenesis.

48

49

50

51 **INTRODUCTION**

52

53 Thyroid hormones (THs) exert a wide variety of effects on lymphocyte function, and

54 their regulation of tumor processes has also been described. Thus, alterations of the

55 thyroid axis during the course of neoplastic illness, as well as the actions of THs on

56 tumor growth, have been suggested. However, the effect of thyroid status on the

57 evolution of tumors is controversial, and the mechanisms involved remain unknown. It

58 has been reported that hypothyroidism can be a risk factor for the development of liver

59 and breast cancer in humans (Reddy et al., 2007). Moreover, the use of levothyroxine, a

60 synthetic T4 hormone commonly used to treat thyroid disease, was associated with a

61 significantly reduced risk of colorectal cancer (Rennert et al., 2010). However, it was

62 also shown that hypothyroid patients have a lower incidence of mammary carcinoma

63 (Cristofanilli et al., 2005), and deprivation of THs decreased the growth rates of solid

64 tumors, while thyroid hormone supplementation increased it (Guernsey et al., 1980;

65 Hercbergs et al., 2010). Prospective studies to date have also yielded conflicting results.

66 In fact, several studies have suggested that subclinical hyperthyroidism increases the

67 risk of certain solid tumors, but spontaneous hypothyroidism delays the onset and

68 reduces the aggressiveness of cancers (Hercbergs et al., 2010). However, a recent meta-

69 analysis showed no association between hypothyroidism and an increased risk for breast

70 cancer (Angelousi et al., 2012). Thus, the heterogeneity of the analyzed studies

71 precludes firm conclusions. Martínez-Iglesias et al. (2009) showed that hypothyroidism

72 resulted in a decreased rate of solid tumor growth, as well as an increase in the

73 development and number of metastases, in murine xenograft models of human

74 hepatocarcinoma and breast cancer. However, low levels of circulating THs, induced by

75 stress, enhanced tumor progression in mice, effect that was reversed following T4

76   administration (Frick et al., 2009). Through *in vitro* studies we have demonstrated that

77   culturing T lymphoma cells for 24 to 72 hours in the presence of THs increased cell

78   proliferation via the activation of intracellular growth-related signaling pathways

79   (Barreiro Arcos et al., 2006 and 2011). However, long term exposure to T4 (15 days of

80   culture or more) leads to T lymphoma cell apoptosis (Mihara et al., 1999, Barreiro

81   Arcos et al., 2013).

82   Cell cycle regulatory proteins such as cyclins, cyclin-dependent kinases (Cdk), Cdk

83   inhibitors (CdkI) and tumor suppressor proteins play important roles in tumor growth

84   and progression. The expression of cyclins D1, D2, D3 are required for the progression

85   from G0 to G1, E2 is necessary for G1 to S phase transition and B1 for G2 to M. These

86   cyclins bind to their corresponding Cdks to form active complexes that induce the

87   expression of a large number of cell cycle regulatory genes. Additionally, tumor

88   suppressor genes inhibit cyclin-Cdks complexes leading to cell cycle arrest.

89   Both TH-mediated up- or down-regulation of cyclins were demonstrated in several

90   tissues (Ledda-Columbano et al., 2005; Verga-Falzacappa et al., 2012; Chattergoon et

91   al., 2007). Also, it has been shown TH-mediated regulation of cyclin-Cdk complexes

92   leqading to cell arrest (Toms et al., 1998) or to cell differentiation (Ballock et al., 2000).

93   Alisi et al. (2005) showed *in vivo* that hyperthyroidism increases the levels of cyclin D1,

94   E and A and the activity of cyclin-cdk complexes, and decreases the levels of cdk

95   inhibitors, such as p16/INK4A and p27/Kip1. Also, they demonstrated that

96   hypothyroidism induces contrary effects and that THs modulate the expression of the

97   tumor suppressor genes p53 and p73, both involved in apoptosis and growth arrest. So

98   the possibility that thyroid status influence tumor growth by altering the expression of

99   cyclin, Cdks, CdkI or tumor suppressor genes deserves to be explored.

100   The development of solid tumors requires the formation of new blood vessels.

101   Numerous studies have demonstrated that the thyroid status modulates angiogenesis, but

102   the results of these studies are controversial. Kucharz et al. (2003) showed that

103   increased or decreased levels of endostatin, a natural inhibitor of angiogenesis, were

104   associated with hyperthyroidism and hypothyroidism, respectively. Additionally,

105   increased serum levels of angiogenic molecules were found in autoimmune thyroid

106   diseases (Figueroa-Vega et al., 2009). The recent description of a plasma membrane

107   receptor for THs that could mediate the proliferative action of the hormone in blood

108   vessels and tumor cells could shed some light on this matter (Cheng et al., 2010).

109   Based on this background, the aim of this work was to study the effects of thyroid status

110   on T cell lymphoma growth *in vivo* in euthyroid, hyperthyroid or hypothyroid syngeneic

111   mice, thus deepening our understanding of the mechanisms involved in TH action,

112   particularly those related to cell cycle progression and tumor angiogenesis.

113

114   **MATERIALS AND METHODS**

115

116   **Animal models**

117

118   Inbred female C57BL/6J (H-2^b) mice, 2-3 months old, were bred and kept at the

119   Instituto de Investigaciones Biomédicas (BIOMED, CONICET-UCA, Buenos Aires,

120   Argentina) in accordance with the ARRIVE Guidelines (Kilkenny et al., 2010). All

121   experimental protocols were approved by the Institutional Committee for the Care and

122   Use of Laboratory Animals, School of Medicine. Animals were kept in a 12-hour light-

123   dark cycle with a controlled temperature between 18 and 22°C, with *ad libitum* access

124   to food and water.

125   Models of hyperthyroidism or hypothyroidism were developed in accordance to Klecha

126   et al. (2005 and 2006). Briefly, hyperthyroidism was achieved by daily treatment with

127   0.012 mg/ml T4 (Sigma-Aldrich, St. Louis, Mo., USA) in the drinking water for 1

128   month, and hypothyroidism by similar treatment with 0.5 mg/ml of propylthiouracil

129   (PTU; Sigma-Aldrich) for 15 days.

130

131   **Hormone determinations**

132

133   Blood was collected from the tail vein using a capillary tube coated with anticoagulant,

134   and plasma was obtained by centrifugation. The plasma levels of T3 and T4 were

135   determined using commercial radioimmunoassay (RIA) kits with specific antibodies

136   (Immunotech, Praga, Czech Republic) according to the manufacturer's instructions. The

137   plasma TSH level was assayed using an ELISA kit (Uscn Life Science Inc., Wuhan,

138   Hubei, Republic of China).

139

140   **Lymphoma model**

141

142   The tumor cell line EL-4 (ATCC, Catalog Number TIB-39), a mouse T-cell lymphoma

143   expressing the $H-2^b$ and Thy-1.2 haplotype, as well as the $CD3^+$ and αβ T-cell receptors;

144   was routinely tested by flow cytometry with specific antibodies against the

145   corresponding surface markers. These cells were cultured at an optimal concentration

146   ($1–5×10^5$ cells/ml) in RPMI-1640 medium supplemented with 10% v/v fetal bovine

147   serum (FBS), 2 mmol l^{-1} glutamine and 100 mg/ml of streptomycin (all from Life

148   Technologies, NY, USA). Euthyroid, hyperthyroid or hypothyroid C57BL/6J syngeneic

149   animals were injected subcutaneously with $3x10^5$ EL-4 cells in 200 μl of PBS to

150   generate a solid tumor. After cell inoculation, hormonal treatments were maintained

151   until the end of the experiments.

152

153   **Tumor development**

154

155   Tumor length and width were measured daily using calipers. Tumor volume was

156   calculated by the equation V= $(\pi/6) \times \text{length} \times \text{width}^2$ (Frick et al., 2011). The rate of

157   tumor growth was quantified by carboxyfluorescein succinimidyl ester (CFSE) staining

158   (Vybrant CFDA SE Cell Tracer Kit, Life Technologies; Lyons et al., 1999). The cells

159   were labeled as previously described (Barreiro Arcos et al., 2006). The stained cells

160   (3×10^5 cells/0.2 ml PBS) were subcutaneously inoculated into C57BL/6J mice with

161   different thyroid status. Ten days later, the mice were sacrificed, and the solid tumors

162   were extracted and dispersed in a metal mesh. The tumor cell suspensions were fixed in

163   3.7 % v/v formaldehyde and analyzed by flow cytometry (BD FACSCalibur) at 492 nm.

164   The estimated cell division time was calculated from the mean fluorescence intensity

165   (MFI) values of the EL-4 cells using the following equation: $T_{1/2} = [$ k x time post-

166   inoculation $] / \ln T - \ln T_0$, where $T_{1/2}$ is the cell doubling time, k is the constant of value

167   0.693, T is the MFI of the CFSE quantified at ten days post-inoculation and T_0 is the

168   MFI of the CFSE of EL-4 cells prior to inoculation (Frick et al., 2009).

169   Animal survival analysis was determined using Kaplan-Meier curves. Briefly, the mice

170   were monitored every day and euthanized according to the guidelines for animal care

171   when they showed signs of suffering, hypothermia and slow locomotion, which is

172   characteristic of animals that are close to death (Massari et al., 2013). All animals had

173   approximately the same tumor burden, without metastatic dissemination when

174   sacrificed.

175 **Tumor histopathology**

176

177 Solid tumors growing in euthyroid, hyperthyroid and hypothyroid mice were excised,

178 and fixed in 3.7 % v/v formaldehyde overnight. Then, the samples were embedded in

179 paraffin and cut into 4 μm thick serial sections using a microtome. Tumor morphology

180 and histopathological characteristics were examined after hematoxylin-eosin (H&E) and

181 Masson's trichrome staining. The number of mitotic cells was quantified as the number

182 of cells with visible chromosomes in 630x magnification fields. Vascularization was

183 determined using Masson's trichrome staining, and the stained sections were screened

184 at 50 x magnification to identify the largest vascular areas around the tumor. In these

185 areas, intratumoral vascularity was evaluated by counting the vessels in 10 random

186 fields from inside the tumor at 630 x magnification. Light microscopy was performed

187 on an Axiolab Karl Zeiss microscope (Göttingen, Germany). Photographs were taken at

188 630 x magnifications using a Canon PowerShot G5 camera (Tokyo, Japan).

189 Intratumoral vascularization was also analyzed by immunohistochemistry.

190

191 **Immunohistochemistry**

192

193 Cell proliferation, apoptosis and angiogenesis markers were examined by

194 immunohistochemistry in tumor tissue sections, prepared as previously described. The

195 antigen retrieval was performed in citrate buffer (10 mmol l^{-1}, pH 6.0) at 100°C, and

196 endogenous peroxidase activity was blocked with 3% v/v H_2O_2 in distilled water. After

197 blocking, the tissues were incubated with the following primary antibodies overnight in

198 a humidified chamber at 4ºC: mouse anti-proliferating cell nuclear antigen (PCNA,

199 1:100, Santa Cruz Biotechnology, Inc., Dallas, Texas, USA), rabbit anti-cleaved

200   caspase-3 (1:100, Abcam, Cambridge, MA, USA) and rabbit anti-CD31 (1:200,

201   Abcam). Immunoreactivity was detected using horseradish peroxidase-conjugated anti-

202   mouse or anti-rabbit antibodies and was visualized by diaminobenzidine staining

203   (Sigma-Aldrich). Serial sections from selected positive cases were used as controls, by

204   replacing the primary antibody with either a normal mouse or rabbit IgG or PBS in the

205   staining procedure. No signal was detected in these control samples.

206

207   **Angiogenesis**

208

209   EL-4 cells ($3x10^5$) were subcutaneously inoculated into the left flank of euthyroid,

210   hyperthyroid and hypothyroid mice. On day 6, when the tumors were palpable in the

211   three groups, mice were sacrificed, and the blood vessels supplying the tumor were

212   quantified using microscopy, as previously described by Ferrando et al. (2011). It is

213   worth noting that it is not possible to accurately evaluate peritumoral angiogenesis at

214   day 10, because of the tumor mass great size. To evaluate the level of angiogenesis

215   associated with the tumor, the number of blood vessels in the tumor tissue area was

216   normalized to the number of vessels in the normal dermal tissue area present in the right

217   flank (control), which was inoculated with sterile PBS solution.

218

219   **Reverse transcription (RT) and real time quantitative polymerase chain reaction**

220   **(qPCR)**

221

222   After the animals were sacrificed, solid tumors were removed and immediately

223   homogenized in Tri-Reagent (Genbiotech SRL, Buenos Aires, Argentina) to isolate the

224   RNA, according to the manufacturer's instructions. The RNA pellets were dissolved in

225   RNase-free water and the RNA concentration was quantified by measuring the

226   absorbance at 260 nm (Nanodrop ND-1000, UK). Complementary DNA (cDNA) was

227   synthesized by retrotranscription using the Omniscript kit (Qiagen, Germantown, MD,

228   USA) following the manufacturer's instructions using 2 μg of total RNA and 1 μmol l^{-1}

229   oligodeoxythymidine$_{12-18}$ (Biodynamics SRL, Buenos Aires, Argentina). The PCR

230   reactions were performed using a commercial master mix for Real-Time PCR

231   containing SYBR Green fluorescent dye (Biodynamics SRL) in a total volume of 25 μl,

232   which contained 10 pmol of each primer and 1μl of cDNA. The reactions were carried

233   out in a Rotor Gene-6000 DNA thermal cycler (Corbett, Life Sciences, Sydney,

234   Australia). The cycling conditions were 95 °C for 15 min, followed by 40 cycles of

235   denaturation at 95 °C for 10 s, annealing at 60 °C for 15 s, and extension at 72 °C for 30

236   s. The primer sequences (Biodynamics SRL), shown in **Table 1**, were designed using

237   the Primer Express software version 3.0 (Applied Biosystems, California, USA).

238   Quantification of the target gene expression was performed using the comparative cycle

239   threshold (C_t) method (Livak and Schmittgen, 2001). An average Ct value was

240   calculated from the duplicate reactions and normalized to the expression of β2-

241   microglobulin, and the ΔΔCt value was then calculated.

242

243   **Immunoblot analysis**

244

245   The tumor mass was excised, and the tissue cells were dissected in a metal mesh. The

246   tumor cells were lysed for 30 min at 4°C in lysis buffer (Barreiro Arcos et al., 2013).

247   After centrifugation at 14,000 g for 15 min at 4°C, whole cell protein extracts obtained

248   (30 μg) were separated by SDS-PAGE on 10% v/v polyacrylamide gels using standard

249   methods (Klecha et al. 2006) and transferred to PVDF membranes. Then the

250   membranes were incubated for 18 h with appropriate dilutions of primary antibodies:

251   mouse anti-PCNA or rabbit anti-cleaved caspase-3 (Abcam, Cambridge, MA, USA),

252   rabbit anti-cyclin D1, mouse anti-cyclin D3 and anti-cyclin E1 antibodies (Cell

253   Signaling Technology, MA, USA), rabbit anti-p16/INK4A, mouse anti-p27/Kip1 and

254   mouse anti-p53 antibodies (Santa Cruz Biotechnology). The membranes were then

255   incubated with anti-rabbit (Abcam) or anti-mouse (Santa Cruz Biotechnology)

256   secondary antibodies conjugated to horseradish peroxidase for 1 h. An enhanced

257   chemiluminescence system (Amersham^{TM} ECL^{TM} Prime Western blotting detection

258   reagent; GE Healthcare, Buckinghamshire, UK) was used to detect the proteins. A

259   rabbit anti-β actin antibody (Santa Cruz Biotechnology) was used as a control for

260   protein loaded. Densitometry analysis of the bands was performed using the ImageJ

261   software (version 5.1, Silk Scientific Corporation, NIH, Bethesda, MA). The

262   densitometry units for the protein bands were normalized to the corresponding β actin

263   bands.

264

265   **Statistical analysis**

266

267   The means of the different experimental groups were analyzed for statistical

268   significance using GraphPad PRISM 4.0 Version for Windows (GraphPad Software

269   Inc., La Jolla, California); a two-way Analysis of Variance (ANOVA) followed by

270   Tukey's post hoc analysis was used to assess statistical significance. The differences

271   between the means were considered significant if $p<0.05$. The results are expressed as

272   the mean ± standard error (SE). Survival curves were created using the Kaplan–Meier

273   method, and the survival rates were compared using the Log-rank test.

274

275   **RESULTS**

276

277   **Thyroid status regulates tumor growth**

278

279   The progression of the EL-4 lymphoma cells growing *in vivo* in syngeneic mice with

280   different thyroid status was evaluated. The plasma levels of T3, T4 and TSH were

281   determined to check the efficacy of the T4 and PTU treatments. The hyperthyroid mice

282   showed high plasma levels of T3 and T4 and low levels of TSH, while the hypothyroid

283   mice showed lower T3 and T4 levels, but higher levels of TSH than the euthyroid mice

284   **(Figure 1 A)**. After EL-4 cells inoculation all animals develop solid tumors. The

285   hyperthyroid mice showed a significant increase in EL-4 lymphoma growth, while the

286   hypothyroid showed no statistically significant differences with respect to the tumors in

287   euthyroid controls **(Figure 1 B, C** and **D)**. Additionally, Kaplan-Meier survival curves

288   **(Figure 1 E)** showed a significant reduction in the survival of the hyperthyroid mice

289   compared to the hypothyroid and euthyroid mice, indicating a worse prognosis. The

290   hyperthyroid mice showed a survival of 50 % at 17.2±1.4* days, while the hypothyroid

291   and euthyroid mice showed a survival of 50% at 22.1±1.5 and 21.3±1.7 days,

292   respectively (*$p < 0.05$ vs. the euthyroid or hypothyroid mice). Because the hyperthyroid

293   animals showed increased tumor development compared to the control and hypothyroid

294   mice, the kinetics of EL-4 cell division were evaluated. For this analysis, EL-4 cells

295   were stained with CFSE prior to inoculation, and the mean fluorescence intensity (MFI)

296   of the CFSE labeled-cells in the tumors was evaluated by flow cytometry, ten days post-

297   inoculation. The EL-4 cells growing in the hyperthyroid mice exhibited a lower MFI

298   than the tumor cells in the control or hypothyroid animals **(Figure 2 A and B)**.

299   Consistent with these findings, the hyperthyroid mice showed an increased rate of cell

12

300   proliferation respect to the euthyroid and hypothyroid mice **(Figure 2C)**. No significant

301   differences were observed between the hypothyroid and euthyroid groups. The increase

302   in the cell division rate that was observed in the hyperthyroid mice could contribute to

303   the rapid tumor growth and the lower survival of these animals.

304

305   **Effects of thyroid status on the histological characteristics of the tumor tissue**

306

307   The histopathological characteristics of the tumor tissue were examined using sections

308   stained with hematoxylin-eosin (H&E) and Masson's trichrome. Tumor sections from

309   all of the experimental groups showed undifferentiated lymphoma cells with aberrant

310   nuclei and marked anisokaryosis and karyorrhexis, as well as the presence of connective

311   tissue trabeculae and infiltrates in the muscle tissue. The tumors from the hyperthyroid

312   mice showed an increased number of mitotic cells, as well as the presence of cystic

313   areas and some levels of necrosis. The tumors from the hypothyroid mice exhibited a

314   lower number of mitotic cells and fewer cystic formations, but areas of diffuse

315   hemorrhage and vascular damage with high levels of necrosis were also observed. The

316   absence of necrosis and a low number of cystic formations were found in the tumors

317   from the euthyroid mice **(Figure 3 A and B)**. Additionally, intratumoral vascularization

318   in the tumor sections was evaluated using the Masson's trichrome staining and

319   immunostaining with an anti-CD31 antibody. The tumors from the hyperthyroid mice

320   exhibited more vascularization, with large vessels and increased expression of the CD31

321   vascular endothelium marker, with respect to those in euthyroid or hypothyroid animals

322   **(Figure 3 A and C)**.

323

324   **Thyroid status modulate tumor angiogenesis**

325

326   Peritumoral angiogenesis was quantified in the three experimental groups 6 days after

327   EL-4 cell inoculation, when the tumors were palpable. The hyperthyroid mice displayed

328   an increased number of blood vessels surrounding the tumor tissue **(Figure 3 D and E)**.

329   Additionally, this group showed a higher angiogenesis level in the normal dermal tissue

330   **(Figure 3 D and F, right flank)**. Non-significant differences were found between the

331   euthyroid and hypothyroid animals.

332

333   **Thyroid status alters the balance between proliferation and apoptosis in the tumor**

334   **cells**

335

336   The balance between the proliferation and apoptosis of the T lymphoma cells in the

337   tumors growing in euthyroid, hyperthyroid or hypothyroid mice was evaluated. The

338   tumors from the hyperthyroid mice highly expressed the PCNA marker and cleaved

339   caspase-3 in the non-necrotic areas of the tumor tissue, as shown by

340   immunohistochemistry analysis **(Figure 4 A)**. The protein levels of both markers were

341   also quantified using western blot analysis. The tumors from the hypothyroid and

342   euthyroid mice showed no significant differences in the levels of PCNA or cleaved

343   caspase-3 **(Figure 4 B and C)**. Because the increase in the level of PCNA was greater

344   than the increase in cleaved caspase-3 within the tumor sample, we determined the ratio

345   between both markers. **Figure 4 D** shows that this ratio was increased in the

346   hyperthyroid mice with respect to the other two groups. These results could explain the

347   observed differences in tumor growth among the animals with different thyroid status.

348

349   **Thyroid status modulates the expression of proteins associated with cell cycle**

350   **progression**

351

352   Because we found that the thyroid status modulates the rate of cell division, the

353   expression levels of several genes related to the regulation and the promotion of the cell

354   cycle were analyzed in the solid tumors growing in mice with different thyroid status.

355   The tumors from the hyperthyroid mice showed increased cyclin D1, D3 and E1 mRNA

356   levels. We found no differences in the levels of cyclin A, B and D2 mRNA at this time.

357   The tumors from the hypothyroid mice showed no significant differences in the mRNA

358   levels of the cyclins with respect to the euthyroid control mice **(Figure 5 A)**.

359   Additionally, we observed increased levels of the cyclin D1 and D3 proteins in the

360   hyperthyroid tumors **(Figure 5 B and C)**. The CdkIs are key regulators of cell cycle

361   progression. Thus, we also evaluated their mRNA expression. Only the expression

362   levels of the p16/INK4A and p27/Kip1 genes were modulated by the thyroid status of

363   the animals carrying the tumor. The tumors from the hypothyroid mice showed

364   increased p16/INK4A mRNA expression with respect to the euthyroid animals and

365   increased p27/Kip1 mRNA expression with respect to the euthyroid or hyperthyroid

366   animals **(Figure 6 A)**. Additionally, the increased expression of these proteins was

367   observed only in the hypothyroid animals, with respect to the hyperthyroid animals,

368   according to the western blot results **(Figure 6 C and D)**. Non-significant differences in

369   the mRNA expression of CdkIs were observed in the solid tumors from the

370   hyperthyroid mice compared to the euthyroid mice **(Figure 6 A)**. However, a decrease

371   in the protein levels of p27/Kip1 was observed by western blot analysis **(Figure 6 C**

372   **and D)**.

373   In the case of the tumor suppressor genes, which protect the cells from malignant

374   transformation by inhibiting cell cycle progression, a significant increase in the mRNA

375   expression of p53 was observed in the tumors from the hypothyroid mice compared to

376   the tumors from the hyperthyroid group **(Figure 6 B)**. This was accompanied by an

377   increase in its protein expression **(Figure 6 C and D)**. The tumors from the

378   hyperthyroid mice showed no significant differences in the mRNA expression of the

379   tumor suppressor genes **(Figure 6 B),** but a decrease in p53 protein, with respect to

380   euthyroid controls, was observed **(Figure 6 C and D)**.

381

382   **DISCUSSION**

383

384   Despite the controversial results on the effect of thyroid status regulation on tumor

385   growth, we show here that the development of T cell lymphoma in syngeneic mice is

386   affected by a thyroid hormone-mediated increase in tumor T cell proliferation. We

387   showed that hyperthyroid mice developed larger tumors than the control or hypothyroid

388   animals, effect that was impaired by reverting to euthyroid conditions (data not shown).

389   This was due to an increased cell proliferation rate. In fact, we have already shown that

390   THs have different effects on the murine BW5147 T lymphoma cell line, depending on

391   the time of exposure. THs increased *in vitro* tumor cell proliferation through the

392   activation of PKCζ and NOS and the increased expression of iNOS when exposed to

393   THs for less than 5 days in culture (Barreiro Arcos et al., 2006). Additionally, we

394   showed that this proliferative activity was mediated by genomic and non-genomic

395   mechanisms involving ERK activation and thyroid hormone receptor regulation

396   (Barreiro Arcos et al., 2011). However, prolonged treatment with THs led to cell death

397   by apoptosis (Barreiro Arcos et al., 2013). Similar findings were observed in the EL-4

16

398   cell line (data not shown). Additionally, other *in vitro* studies in human breast cancer

399   lines (Tang et al., 2004), papillary and follicular thyroid cells (Lin et al., 2007), glioma

400   U-87 MG cells (Lin et al., 2009) and lung cancer cells (Meng et al., 2011) showed that

401   exposure to physiological concentrations of T3 and T4 induced cell proliferation

402   through the activation of ERK1/2.

403   Moreover, the tumor-bearing hyperthyroid mice exhibited a decreased survival rate. The

404   increased cell division rate that was observed in the tumors from the hyperthyroid mice

405   could contribute to the rapid tumor growth and the reduced survival of these animals. It

406   is unlikely that animals died as a result of the effects of hyperthyroidism, as

407   hyperthyroid animals without tumor live for significantly greater time than the tumor-

408   bearing animals. However, we cannot rule out that the stress generated by the tumor

409   development could negatively influence the survival of hyperthyroid animals (Frick et

410   al., 2009).

411   No differences were observed between the tumors grown in the euthyroid and

412   hypothyroid mice.

413   The balance between the proliferation and apoptosis of the tumor cells is considered an

414   indicator of tumor growth; therefore, we analyzed these parameters in our animal

415   models. An increased number of cells expressing the PCNA cell proliferation marker

416   and active caspase-3 were found in the tumors from the hyperthyroid animals with

417   respect to the controls, and the ratio between the levels of these proteins was also higher

418   in the hyperthyroid mice. Additionally, we observed a significant increase in the

419   number of mitotic cells in the H&E-stained tissue sections of the hyperthyroid tumors,

420   as well as localized phenomena of apoptosis that could be observed as cystic areas

421   without cellular content. This last observation could be explained because the fast speed

422   of cell proliferation may cause an insufficient arrival of nutrients and oxygen to the

17

423   tumor tissue inducing apoptotic areas. Both phenomena occur together, but our results

424   indicate that the proliferative effect is stronger than the apoptotic action, which is in

425   agreement with the increased tumor growth observed in this group.

426   Neovascularization is an essential process for the survival of tumor cells and tumor

427   growth. We next examined peritumoral and intratumoral angiogenesis in the tumors

428   from the euthyroid, hyperthyroid and hypothyroid mice. Peritumoral angiogenesis was

429   quantified in the tumors grown in our experimental models 6 days after EL-4 cell

430   inoculation, when the tumor volume was only a few millimeters. The tumors from the

431   hyperthyroid mice showed a greater irrigation of blood vessels than the tumors from the

432   euthyroid or hypothyroid animals. Additionally, the hyperthyroid mice displayed an

433   increased number of blood vessels in the contralateral flank, which was not inoculated

434   with tumor cells. It is worth to notice that hypothyroid mice showed greater levels of

435   necrosis in their tumors than the other studied groups, despite having similar levels of

436   angiogenesis to those observed in euthyroid animals. Similar results were obtained by

437   Martinez et.al (2009), who showed that the reduced tumor volume in hypothyroid hosts

438   correlated with a lower proliferation of the tumors, which was accompanied also by

439   enlargement of the necrotic area of the tumors. This is probably as a result of THs

440   deficiency. In fact, THs are necessary growth factors involved in T cell lymphoma

441   proliferative and survival signals (Barreiro Arcos et. al, 2006 and 2011), so the lack of

442   THs would induce cell death signaling that leads to the formation of the necrotic areas

443   observed in these tumors.

444   Intratumoral vascularity was evaluated by counting the blood vessels inside the tumor

445   10 days after inoculation with the tumor cells. The tumor tissue from the hyperthyroid

446   animals showed a larger number of endothelial cells (CD31+), which was in agreement

447   with the increased number of blood vessels shown by Masson's trichrome staining. The

448   hypothyroid mice displayed similar levels of intratumoral and peritumoral angiogenesis

449   as the euthyroid controls. Our results are supported by numerous works that suggest the

450   involvement of the THs in the modulation of angiogenesis. Patients with Grave's

451   disease have high serum levels of angiogenic molecules, which are significantly

452   decreased after treatment with antithyroid drugs (Figueroa-Vega et al., 2009).

453   Additionally, patients with Grave's disease exhibit an increased microvessel density

454   (Tseleni-Balafouta et al., 2006) and angiogenic vascular endothelial growth factor

455   serum levels (Iitaka et al., 1998).

456   We showed that the hyperthyroid state induces tumor growth by accelerating the

457   process of cell division. There is evidence that the THs modulate the progression of the

458   cell cycle through the regulation of cell cycle regulatory proteins (Woodmansee et al.,

459   2006). We observed that the levels of cyclins D1 and D3 were increased in the tumors

460   grown in the hyperthyroid animals. Increased cyclin D1, which regulates the entry into

461   G1 phase of the cell cycle, has been widely linked to the regulation of the cell cycle by

462   THs in various cell types (Verga Falzacappa et al., 2012; Ledda-Columbano et al.,

463   2006; Zhang et al., 2012). Several pieces of evidence have indicated that cyclins D1 and

464   D3 are involved in T-cell lymphomagenesis and are important molecular markers of

465   oncogenic potential in T cell lymphomas (Cheng et al., 2008; Teramoto et al., 1999).

466   Furthermore, cyclin D3 overexpression is associated with a higher proliferation rate, as

467   well as with lower p27/Kip1 and altered p53 expression (Møller et al., 2001). The

468   positive regulation of cyclins D1 and D3 has been associated with a poor prognosis in

469   patients with lymphoma (Zukerberg et al., 1995; Kanavaros et al., 2001; Mao et al.,

470   2006). Cyclin E1 is a key mediator of T-cell lymphomagenesis and regulates the

471   transition between G1 and S phases (Geisen et al., 2003; Karsunky et al., 1999;

472   Hosokawa et al., 1995; Kang-Decker et al., 2004); however, we observed an increase

473   only of the mRNA expression of cyclin E in the hyperthyroid animals, but we cannot

474   rule out an increment of its protein levels at other time points. Hypothyroidism does not

475   affect the expression pattern of the cyclins, as the cell division speed and tumor growth

476   were similar to the tumors grown in the euthyroid animals.

477   Previous reports indicated that the INK4 family is altered in lymphoma (Gallardo et al.,

478   2004; Baur et al., 1999; Nagasawa et al., 2006). We observed an increase in the mRNA

479   and protein levels of p16/INK4A in the tumors from the hypothyroid mice compared to

480   those from the hyperthyroid mice, but no significant differences were observed in

481   p15/INK4B expression. The expression levels of p21/Cip1 were not modulated by

482   thyroid status, even though it has been suggested that this protein is involved in the

483   development of T cell lymphoma (Kanavaros et al., 2001), but we observed a decreased

484   expression of p27/Kip1 in the tumors from the hyperthyroid animals compared to those

485   from the hypothyroid animals, which is in agreement with several pieces of

486   experimental evidence. In this regard, Cheng et al., (2008) found that p27/Kip1

487   deficiency in transgenic mice leads to T-cell hyperplasia and the development of

488   spontaneous T lymphomas, and Geisen et al., (2003) showed that the reduction in

489   p27/Kip1 expression is involved in the T cell lymphomagenesis.

490   Additionally, we evaluated the expression of the PTEN, Rb and p53 tumor suppressor

491   genes, whose expression levels are often deregulated in T cell lymphomas (Kanavaros et

492   al., 2001; Mao et al., 2006; Møller et al., 2002). We only observed a decrease in the

493   expression of p53 in the tumors from the hyperthyroid animals compared to those from the

494   hypothyroid or euthyroid animals, and this result was anticipated due to its key role in

495   hematological malignancies (Kanavaros et al., 2001; Møller et al., 2002). The decreased

496   expression of the p16/INK4A, p27/Kip1 and p53 proteins in the tumors from the

497   hyperthyroid mice could facilitate cell cycle progression and contribute to tumor

498   growth.

499   The results shown in this work are in agreement with *in vivo* studies investigating the

500   modulation of cell cycle regulators in other physiological, non-neoplastic processes.

501   Alisi et al. (2005) demonstrated that hyperthyroidism increased the expression of cyclins

502   D1, E and A and decreased the expression of p16/INK4A and p27/Kip1 in a rat model of

503   liver regeneration; this study also showed that hypothyroidism resulted in the reduced

504   expression of these cyclins, as well as the increased expression of p16/INK4A, p27/Kip1

505   and p53.

506   Based on these results, we conclude that thyroid status can modulate T lymphoma EL-4

507   growth through the regulation of cell cycle protein expression, which includes the

508   cyclins, cyclin-dependent kinase inhibitors, and tumor suppressor genes, and through

509   the up-regulation of angiogenesis. These results will contribute to a better understanding

510   of the actions of THs during tumor development.

511

512   **DECLARATION OF INTEREST**

513

514   There is no conflict of interest that could be perceived as prejudicing the impartiality of

515   the research reported

516

517   **FUNDING**

518

521   Promoción Científica y Técnica, PICT 2008 Nº 1858 and PICT Raíces 2012 Nº 1328;

522   and the Universidad de Buenos Aires, UBACYT Nº 20020100100291.

523

528

529

530   **REFERENCES**

531

532   Alisi A, Demori I, Spagnuolo S, Pierantozzi E, Fugassa E & Leoni S 2005 Thyroid

533   status affects rat liver regeneration after partial hepatectomy by regulating cell cycle and

534   apoptosis. *Cellular Physiology and Biochemistry* **15**(1-4) 69-76.

535

536   Angelousi AG, Anagnostou VK, Stamatakos MK, Georgiopoulos GA & Kontzoglou

537   KC 2012 Primary HT and risk for breast cancer: a systematic review and meta-

538   analysis. *European Journal of Endocrinology* **166** 373–381.

539

540   Ballock RT, Zhou X, Mink LM, Chen DH, Mita BC & Stewart MC 2000 Expression of

541   cyclin-dependent kinase inhibitors in epiphyseal chondrocytes induced to terminally

542   differentiate with thyroid hormone. *Endocrinology* **141**(12) 4552-4557.

543

544   Barreiro Arcos ML, Gorelik G, Klecha A, Genaro AM & Cremaschi GA 2006 Thyroid

545   hormones increase inducible nitric oxide synthase gene expression downstream from

546   PKC-zeta in murine tumor T lymphocytes. *American Journal of Physiology. Cell*

547   *Physiology* **291**(2) 327-336.

548

549   Barreiro Arcos ML, Sterle H, Paulazo MA, Valli E, Klecha AJ, Isse B, Pellizas CG,

550   Farías RN & Cremaschi GA 2011 Cooperative nongenomic and genomic actions on

551   thyroid hormone mediated-modulation of T cell proliferation involve up-regulation of

552   thyroid hormone receptor and inducible nitric oxide synthase expression. *Journal of*

553   *Cell Physiology* **226**(12) 3208-3218.

554

555   Barreiro Arcos ML, Sterle HA, Vercelli C, Valli E, Cayrol MF, Klecha AJ, Paulazo

556   MA, Diaz Flaqué MC, Franchi AM & Cremaschi GA 2013 Induction of apoptosis in T

557   lymphoma cells by long-term treatment with thyroxine involves PKCζ nitration by

558   nitric oxide synthase. *Apoptosis* **18**(11) 1376-1390.

559

560   Baur AS, Shaw P, Burri N, Delacrétaz F, Bosman FT & Chaubert P 1999 Frequent

561   methylation silencing of p15(INK4b) (MTS2) and p16(INK4a) (MTS1) in B cell and T-

562   cell lymphomas. *Blood* **94** 1773–1781.

563

564   Chattergoon NN, Giraud GD & Thornburg KL 2007 Thyroid hormone inhibits

565   proliferation of fetal cardiac myocytes in vitro. *Journal of Endocrinology* **192**(2) R1-8.

566

567   Cheng N, Van de Wetering CI & Knudson CM 2008 p27 deficiency cooperates with

568   Bcl-2 but not Bax to promote T-cell lymphoma. *PLoS One* **3**(4) e1911.

569

570   Cheng SY, Leonard LJ & Davis PJ 2010 Molecular aspects of thyroid hormone actions.

571   *Endocrine Reviews* **31** 139–170.

572 Cristofanilli M, Yamamura Y, Kau SW, Bevers T, Strom S, Patangan M, Hsu L,

573 Krishnamurthy S, Theriault RL & Hortobagyi GN 2005 Thyroid hormone and breast

574 carcinoma. Primary hypothyroidism is associated with a reduced incidence of primary

575 breast carcinoma. *Cancer* **103**(6) 1122-1128.

576

577 Figueroa-Vega N, Sanz-Cameno P, Moreno-Otero R, Sánchez-Madrid F, González-

578 Amaro R & Marazuela M 2009 Serum levels of angiogenic molecules in autoimmune

579 thyroid diseases and their correlation with laboratory and clinical features. *The Journal*

580 *of Clinical Endocrinology & Metabolism* **94**(4) 1145-1153.

581

582 Frick LR, Arcos ML, Rapanelli M, Zappia MP, Brocco M, Mongini C, Genaro AM &

583 Cremaschi GA 2009 Chronic restraint stress impairs T-cell immunity and promotes

584 tumor progression in mice. *Stress* **12**(2) 134-143.

585

586 Ferrando M, Gueron G, Elguero B, Giudice J, Salles A, Leskow FC, Jares-Erijman EA,

587 Colombo L, Meiss R, Navone N, De Siervi A, Vazquez E 2011 Heme oxygenase 1

588 (HO-1) challenges the angiogenic switch in prostate cancer. *Angiogenesis* **14**(4) 467-

589 479.

590

591 Frick LR, Rapanelli M, Arcos ML, Cremaschi GA & Genaro AM 2011 Oral

592 administration of fluoxetine alters the proliferation/apoptosis balance of lymphoma cells

593 and up-regulates T cell immunity in tumor-bearing mice. *European Journal of*

594 *Pharmacology* **659**(2-3) 265-272.

595

596   Frick LR, Rapanelli M, Bussmann U, Klecha AJ, Barreiro Arcos ML, Genaro AM &

597   Cremaschi GA 2009 Involvement of thyroid hormones in the alterations of T-cell

598   immunity and tumor progression induced by chronic stress. *Biological Psychiatry*

599   **65**(11) 935-942.

600

601   Gallardo F, Esteller M, Pujol RM, Costa C, Estrach T & Servitje O 2004 Methylation

602   status of the p15, p16 and MGMT promoter genes in primary cutaneous T-cell

603   lymphomas. *Haematologica* **89** 1401–1403.

604

605   Geisen C, Karsunky H, Yücel R & Möröy T 2003 Loss of p27(Kip1) cooperates

606   with cyclin E in T-cell lymphomagenesis. *Oncogene* **22** 1724–1729.

607

608   Guernsey DL, Ong A & Borek C 1980 Thyroid hormone modulation of X-ray induced

609   in vitro neoplastic transformation. *Nature* **288** 591–592.

610

611   Hercbergs AH, Ashur-Fabian O & Garfield D 2010 Thyroid hormones and cancer:

612   clinical studies of hypothyroidism in oncology. *Current Opinion in Endocrinology,*

613   *Diabetes and Obesity* **17** 432–436.

614

615   Hosokawa Y, Yang M, Kaneko S, Tanaka M & Nakashima K 1995 Synergistic gene

616   expressions of cyclin E, cdk2, cdk5 and E2F-1 during the prolactin-induced G1/S

617   transition in rat Nb2 pre-T lymphoma cells. *Biochemistry and Molecular Biology*

618   International **37** 393–399.

619

620 Iitaka M, Miura S, Yamanaka K, Kawasaki S, Kitahama S, Kawakami Y, Kakinuma S,

621 Oosuga I, Wada S & Katayama S 1998 Increased serum vascular endothelial growth

622 factor levels and intrathyroidal vascular area in patients with Graves' disease and

623 Hashimoto's thyroiditis. *The Journal of Clinical Endocrinology and Metabolism* **83**(11)

624 3908-3912.

625

626 Kanavaros P, Bai M, Stefanaki K, Poussias G, Rontogianni D, Zioga E, Gorgoulis V, &

627 Agnantis NJ 2001 Immunohistochemical expression of the p53,mdm2, p21/Waf-1, Rb,

628 p16, Ki67, cyclin D1, cyclin A and cyclin B1 proteins and apoptotic index in T-cell

629 lymphomas. *Histology and Histopathology* **16** 377–386.

630

631 Kang-Decker N, Tong C, Boussouar F, Baker DJ, Xu W, Leontovich AA, Taylor WR,

632 Brindle PK & Van Deursen JM 2004 Loss of CBP causes T cell lymphomagenesis in

633 synergy with p27Kip1 insufficiency. *Cancer Cell* **5** 177–189.

634

635 Karsunky H, Geisen C, Schmidt T, Haas K, Zevnik B, Gau E & Möröy T 1999

636 Oncogenic potential of cyclin E in T-cell lymphomagenesis in transgenic mice:

637 evidence for cooperation between cyclin E and Ras but not Myc. *Oncogene* **18** 7816 -

638 7824.

639

640 Kilkenny C, Browne WJ, Cuthill IC, Emerson M & Altman DG 2010 Improving

641 Bioscience Research Reporting: The ARRIVE Guidelines for Reporting Animal

642 Research. *PLoS Biol* **8**(6) e1000412. doi:10.1371/journal.pbio.1000412

643

644 Klecha AJ, Barreiro Arcos ML, Genaro AM, Gorelik G, Silberman DM, Caro R &

645 Cremaschi GA 2005 Different mitogen-mediated Beta-adrenergic receptor modulation

646 in murine T lymphocytes depending on the thyroid status. *Neuroimmunomodulation*

647 **12**(2) 92-99.

648

649 Klecha AJ, Genaro AM, Gorelik G, Barreiro Arcos ML, Silberman DM, Schuman M,

650 Garcia SI, Pirola C & Cremaschi GA 2006 Integrative study of hypothalamus-pituitary-

651 thyroid-immune system interaction: thyroid hormone-mediated modulation of

652 lymphocyte activity through the protein kinase C signaling pathway. *Journal of*

653 *Endocrinology* **189**(1) 45-55.

654

655 Kucharz EJ, Kotulska A, Kopeć M, Stawiarska-Pieta B & Pieczyrak R 2003 Serum

656 level of the circulating angiogenesis inhibitor endostatin in patients with

657 hyperthyroidism or hypothyroidism. *Wiener klinische Wochenschrift 115*(5-6) 179-181.

658

659 Ledda-Columbano GM, Molotzu F, Pibiri M, Cossu C, Perra A & Columbano A 2006

660 Thyroid hormone induces cyclin D1 nuclear translocation and DNA synthesis in adult

661 rat cardiomyocytes. *FASEB Journal* **20**(1) 87-94.

662

663 Ledda-Columbano GM, Perra A, Pibiri M, Molotzu F & Columbano A 2005 Induction

664 of pancreatic acinar cell proliferation by thyroid hormone. *Journal of Endocrinology*

665 **185**(3) 393-9.

666

667 Lin HY, Sun M, Tang HY, Lin C, Luidens MK, Mousa SA, Incerpi S, Drusano GL,

668 Davis FB & Davis PJ 2009 L-Thyroxine vs. 3,5,3'-triiodo-L-thyronine and cell

669   proliferation: activation of mitogen-activated protein kinase and phosphatidylinositol 3-

670   kinase. *American Journal of Physiology Cell Physiology* **296**(5) 980-991.

671

672   Lin HY, Tang HY, Shih A, Keating T, Cao G, Davis PJ & Davis FB 2007 Thyroid

673   hormone is a MAPK-dependent growth factor for thyroid cancer cells and is anti-

674   apoptotic. *Steroids* **72**(2) 180-187.

675

676   Livak KJ & Schmittgen TD 2001 Analysis of relative gene expression data using real-

677   time quantitative PCR and the 2(-Delta Delta C(T)) Method. *Methods* **25**(4) 402-408.

678

679   Lyons AB 1999 Divided we stand: tracking cell proliferation with carboxyfluorescein

680   diacetate succinimidyl ester. *Immunology and Cell Biology* **77** 509-515.

681

682   Mao X, Orchard G, Vonderheid EC, Nowell PC, Bagot M, Bensussan A, Russell-Jones

683   R, Young BD & Whittaker SJ 2006 Heterogeneous abnormalities of CCND1 and RB1

684   in primary cutaneous T-Cell lymphomas suggesting impaired cell cycle control in

685   disease pathogenesis. *Journal of Investigative Dermatology* **126** 1388-1395.

686

687   Martínez-Iglesias O, García-Silva S, Regadera J & Aranda A 2009 Hypothyroidism

688   enhances tumor invasiveness and metastasis development. *PLoS One* **4**(7) e6428.

689

690   Massari NA, Medina VA, Cricco GP, Martinel Lamas DJ, Sambuco L, Pagotto R,

691   Ventura C, Ciraolo PJ, Pignataro O, Bergoc RM & Rivera ES 2013 Antitumor activity

692   of histamine and clozapine in a mouse experimental model of human melanoma.

693   *Journal of Dermatological Science* **72**(3) 252-262.

694   Meng R, Tang HY, Westfall J, London D, Cao JH, Mousa SA, Luidens M, Hercbergs

695   A, Davis FB, Davis PJ & Lin HY 2011 Crosstalk between integrin αvβ3 and estrogen

696   receptor-α is involved in thyroid hormone-induced proliferation in human lung

697   carcinoma cells. *PLoS One* **6**(11) e27547.

698

699   Mihara S, Suzuki N, Wakisaka S, Sekita N, Hoshino T & Sakane T 1999 Effects of

700   thyroid hormones on apoptotic cell death of human lymphocytes. *The Journal of*

701   *Clinical Endocrinology and Metabolism* **84** 1378-1385.

702

703   Møller MB, Nielsen O & Pedersen NT 2001 Cyclin D3 expression in non-Hodgkin

704   lymphoma. Correlation with other cell cycle regulators and clinical features. *American*

705   *Journal of Clinical Pathology* **115**(3) 404-412.

706

707   Møller MB, Nielsen O & Pedersen NT 2002 Frequent alteration of MDM2 and p53 in

708   the molecular progression of recurring non-Hodgkin's lymphoma. *Histopathology* **41**

709   322-330.

710

711   Nagasawa T, Zhang Q, Raghunath PN, Wong HY, El-Salem M, Szallasi A, Marzec M,

712   Gimotty P, Rook AH, Vonderheid EC, Odum N & Wasik MA 2006 Multi-gene

713   epigenetic silencing of tumor suppressor genes in T-cell lymphoma cells; delayed

714   expression of the p16 protein upon reversal of the silencing. *Leukemia Research* **30**

715   303-312.

716

717   Reddy A, Dash C, Leerapun A, Mettler TA, Stadheim LM, Lazaridis KN, Roberts RO

718   & Roberts LR 2007 Hypothyroidism: a possible risk factor for liver cancer in patients

719 with no known underlying cause of liver disease. *Clinical Gastroenterology and*

720 *Hepatology* **5**(1) 118-123.

721

722 Rennert G, Rennert HS, Pinchev M & Gruber SB 2010 A case–control study of

723 levothyroxine and the risk of colorectal cancer. *Journal of the National Cancer Institute*

724 **102** 568–572.

725

726 Tang HY, Lin HY, Zhang S, Davis FB & Davis PJ 2004 Thyroid hormone causes

727 mitogen-activated protein kinase-dependent phosphorylation of the nuclear estrogen

728 receptor. *Endocrinology* **145**(7) 3265-3272.

729

730 Teramoto N, Pokrovskaja K, Szekely L, Polack A, Yoshino T, Akagi T & Klein G

731 1999 Expression of cyclin D2 and D3 in lymphoid lesions. *International Journal of*

732 *Cancer* **81** 543–850.

733

734 Toms SA, Hercbergs A, Liu J, Kondo S, Haqqi T, Casey G, Iwasaki K, Barnett GH &

735 Barna BP 1998 Antagonist effect of insulin-like growth factor I on protein kinase

736 inhibitor-mediated apoptosis in human glioblastoma cells in association with bcl-2 and

737 bcl-xL. *Journal of Neurosurgery* **88**(5) 884-889.

738

739 Tseleni-Balafouta S, Kavantzas N, Balafoutas D & Patsouris E 2006 Comparative study

740 of angiogenesis in thyroid glands with Graves disease and Hashimoto's thyroiditis.

741 *Applied Immunohistochemistry & Molecular Morphology* **14**(2) 203-207.

742

743   Verga Falzacappa C, Timperi E, Bucci B, Amendola D, Piergrossi P, D'Amico D,

744   Santaguida MG, Centanni M & Misiti S 2012 T(3) preserves ovarian granulosa cells

745   from chemotherapy-induced apoptosis. *Journal of Endocrinology* **215**(2) 281-9.

746

747   Woodmansee WW, Kerr JM, Tucker EA, Mitchell JR, Haakinson DJ, Gordon DF,

748   Ridgway EC & Wood WM 2006 The proliferative status of thyrotropes is dependent on

749   modulation of specific cell cycle regulators by thyroid hormone. *Endocrinology* **147**(1)

750   272-282.

751

752   Zhang B, Zhang A, Zhou X, Webb P, He W & Xia X 2012 Thyroid hormone analogue

753   stimulates keratinocyte proliferation but inhibits cell differentiation in epidermis.

754   *International Journal of Immunopathology and Pharmacology* **25**(4) 859-869.

755

756   Zukerberg LR, Yang WI, Arnold A & Harris NL 1995 Cyclin D1 expression in non-

757   Hodgkin's lymphomas. Detection by immunohistochemistry. *American Journal of*

758   Clinical *Pathology* **103** 756-760.

759

760

761

762

763

764

765

766

767

768   **LEGENDS FOR FIGURES**

769

770   **Figure 1: Effects of thyroid status on tumor progression**. The plasma levels of

771   thyroid hormones in euthyroid, hyperthyroid and hypothyroid mice were determined

772   using an ELISA, as described in Materials and Methods **(A)**. Euthyroid, hyperthyroid

773   and hypothyroid mice were subcutaneously inoculated with 3×10^5 EL-4 cells, and the

774   volumes of the resulting solid tumors were measured **(B)**. Representative photographs

775   of the solid tumors grown in mice with different thyroid statuses 10 days after

776   inoculation are shown **(C)**. The tumor tissue weight removed at 10 days post-

777   inoculation was determined **(D)**. Kaplan-Meier survival analysis was performed on the

778   experimental groups subcutaneously inoculated with 3×10^5 EL-4 cells **(E)**. The values

779   are expressed as the mean ± SE. *$p < 0.05$ vs. the corresponding euthyroid mice.

780

781   **Figure 2: Effects of thyroid status on the rate of tumor cell division.** EL-4 cells

782   were stained with carboxyfluorescein diacetate succinimidyl ester (CFSE) and were

783   subcutaneously inoculated into euthyroid, hyperthyroid and hypothyroid mice. Ten

784   days post-inoculation, the tumor tissue was removed, and the CFSE mean fluorescence

785   intensities (MFIs) of the tumor cells were quantified using flow cytometry.

786   Representative histograms of 4 independent experiments are shown. The histogram

787   corresponding to T_0 represents the CFSE fluorescence intensity of the EL-4 cells prior

788   to inoculation into the animal models. The MFIs of the EL-4 cells grown in the

789   euthyroid, hyperthyroid and hypothyroid mice are indicated in parentheses **(A)**. The

790   MFI of each experimental group is shown in the bar graph as a percentage of the MFI

791   at T_0 **(B)**. The estimated cell division time is indicated in the table **(C)**. The values are

792   expressed as the mean ± SE. *$p < 0.01$ vs. the euthyroid mice.

793   **Figure 3: Effects of thyroid status on the histological characteristics of the tumor**

794   **tissue and tumor angiogenesis.** Solid tumors grown in euthyroid, hyperthyroid and

795   hypothyroid mice were excised 10 days after tumor inoculation. The tumor tissue were

796   fixed, embedded in paraffin and cut into serial sections using a microtome. Histological

797   characteristics of the tumor tissue were examined in the tissue sections after staining

798   with hematoxylin-eosin (H&E) and Masson's trichrome. Vascularization in the tissue

799   sections was evaluated using Masson's trichrome and immunostaining with an anti-

800   CD31 antibody. Representative photographs from 4 independent trials using 5 animals

801   per group are shown. The black arrows indicate the mitotic cells (H&E staining), blood

802   vessels (Masson's trichrome) or endothelial cells (CD31+ immunostaining), and the

803   white arrows indicate the hemorrhagic areas (H&E staining) **(A)**. The number of

804   mitotic cells in the tissue sections stained with H&E was quantified. Ten random fields

805   from each sample from each experimental group were analyzed **(B)**. The number of

806   blood vessels in the tissue sections stained with Masson's trichrome solution was

807   quantified. Intratumoral vascularity was evaluated by counting the number of blood

808   vessels inside the tumor in 10 random fields **(C)**. Angiogenesis was quantified in the

809   solid tumors grown in euthyroid, hyperthyroid and hypothyroid mice 6 days after

810   inoculation with EL-4 cells, as described in Materials and Methods. Representative

811   solid tumors irrigated by blood vessels are shown (left flank). The right flanks of the

812   mice without tumor inoculation are shown as controls **(D)**. The number of blood

813   vessels in the tumor tissue area was normalized to the number of vessels in the normal

814   dermal tissue area present in the flank control, which was inoculated with sterile PBS

815   solution **(E)**. The average number of blood vessels in the control flank (without tumor)

816   is shown in the bar graph **(F)**. The values are expressed as the mean ± SE. **p<0.01 or

817   *p<0.05 vs. the euthyroid mice or hyperthyroid mice.

818   **Figure 4: Effects of thyroid status on the cellular proliferation and apoptosis of**

819   **the tumor tissue**. Tumor tissue sections from euthyroid, hyperthyroid or hypothyroid

820   mice excised 10 days after EL-4 cell inoculation. Lymphoma cell proliferation and

821   apoptosis were determined by immunohistochemistry using PCNA or active caspase-3

822   antibodies. Representative photographs from 4 independent experiments using 5

823   animals per group are shown **(A)**. PCNA and active caspase-3 expression was

824   evaluated by western blot analysis from the tumor tissue protein extracts. Actin was

825   used as a protein loading control. The results are representative of 4 independent

826   experiments **(B)**. Densitometric results of the western blot analysis are shown in the bar

827   graph **(C)**. The ratio of PCNA and caspase-3 protein expression is shown **(D)**. The

828   values are expressed as the mean ± SE. *p<0.05 or **p<0.01 vs. the euthyroid mice.

829

830   **Figure 5: Effects of thyroid status on the expression of cell cycle regulatory**

831   **proteins.** Differential gene expression of the cyclins was observed in the tumor tissues

832   from the euthyroid, hyperthyroid and hypothyroid mice. The mRNA expression of the

833   cyclins was determined using qPCR, and the expression levels were normalized to the

834   expression of the housekeeping gene β-actin; the ΔΔCt method was used to calculate

835   fold change **(A)**. The expression of the cyclin proteins was evaluated using western blot

836   analysis. Actin was used as a protein loading control. The results are representative of 4

837   independent experiments **(B)**. Densitometric results of the western blot analysis in the

838   euthyroid, hyperthyroid and hypothyroid mice are shown in the bar graph **(C)**. The

839   values are expressed as the mean ± SE. *p<0.05 or **p<0.01 vs. the euthyroid mice.

840

841   **Figure 6: Effect of thyroid status on cyclin inhibitors and tumor suppressor**

842   **proteins.** The mRNA expression of the cyclin-dependent kinase inhibitors

34

843   (P15/INK4B, p16/INK4A, p21/Cip1 and p27/Kip1) was determined in the tumor

844   tissues from the euthyroid, hyperthyroid and hypothyroid mice using qPCR analysis.

845   Gene expression was normalized to the expression of the β-actin gene, and the ΔΔCt

846   method was used to calculate fold change **(A)**. The mRNA expression of the tumor

847   suppressor genes (p53, PTEN and Rb) as determined using qPCR analysis; expression

848   was normalized to the expression of the β-actin gene, and the ΔΔCt method was used to

849   calculate fold change **(B)**. Protein expression of the cyclin-dependent kinase inhibitors

850   and the tumor suppressor proteins was analyzed using western blot analysis. Actin was

851   used as a protein loading control. The results are representative of 4 independent

852   experiments **(D)**. Densitometric results of the western blot analysis are shown in the bar

853   graph **(E)**. The values are expressed as the mean ± SE. $*p<0.05$ vs. the euthyroid

854   animals; $\#p<0.05$ or $\#\#p<0.01$ vs. the hyperthyroid animals.

855

856

857

858

859

860

861

862

863

864

865

866

867

Figure 1

A

Thyroid status	T3 (ng/100 ml)	T4 (μg/100 ml)	TSH (ng/ml)
Euthyroid	115.0±12.5	5.5±0.7	47.8±5.4
Hyperthyroid	423.0±47.1*	32.7±1.8*	<20
Hypothyroid	60.6±10.2*	<1.0	64.2±6.8*

B

C

D

E
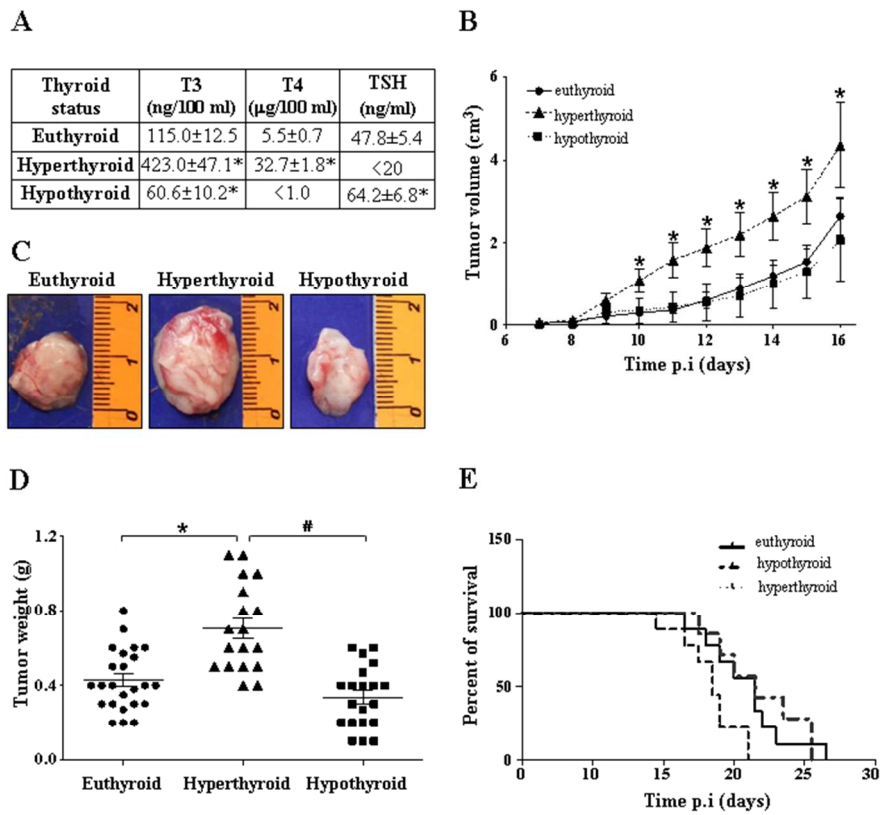
Effects of thyroid status on tumor progression
190x254mm (96 x 96 DPI)

Figure 2

A

B

C

Experimental groups	Cell division time
Euthyroid	40.9±3.7
Hyperthyroid	32.4*±2.9
Hypothyroid	43.9±4.1
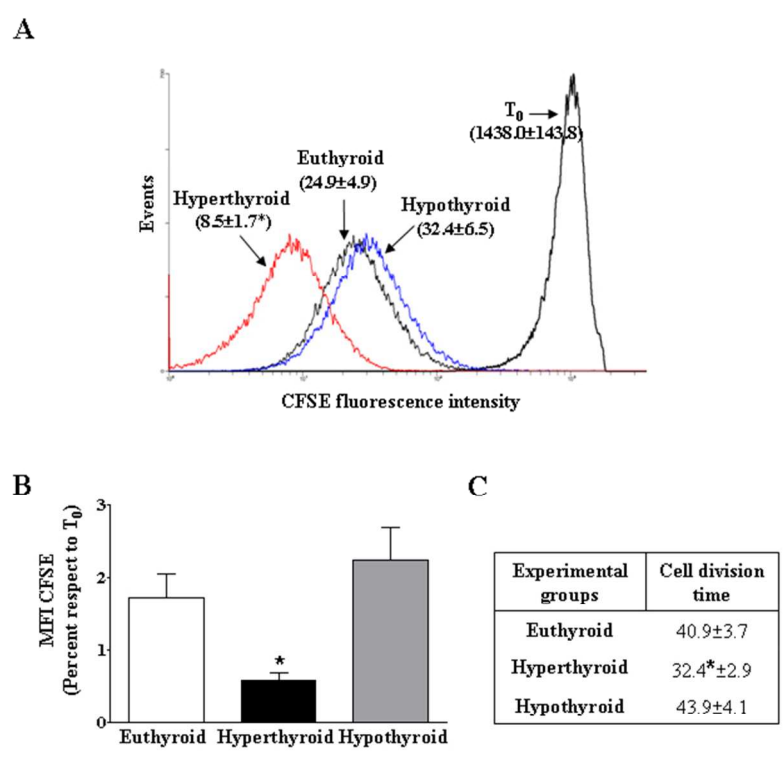
Effects of thyroid status on the rate of tumor cell division
190x254mm (96 x 96 DPI)
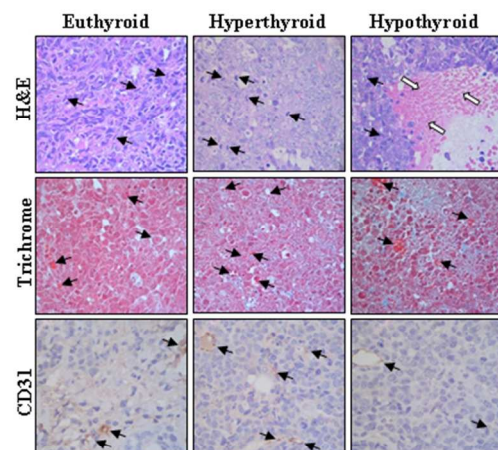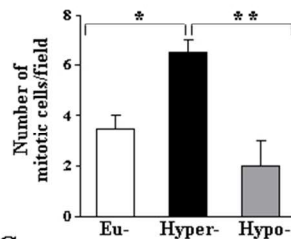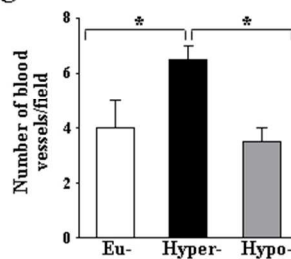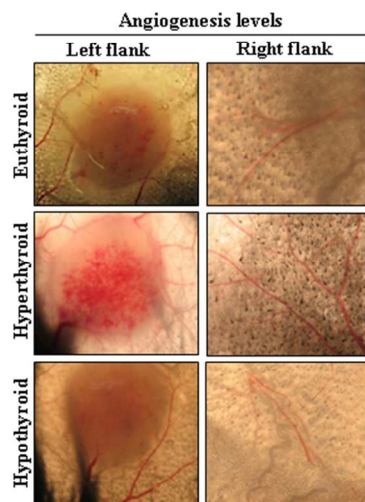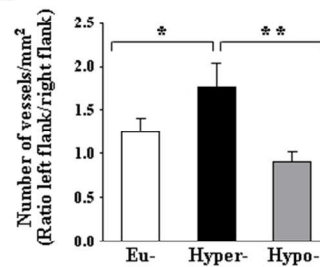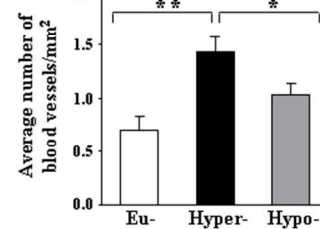
Effects of thyroid status on the histological characteristics of the tumor tissue and tumor angiogenesis
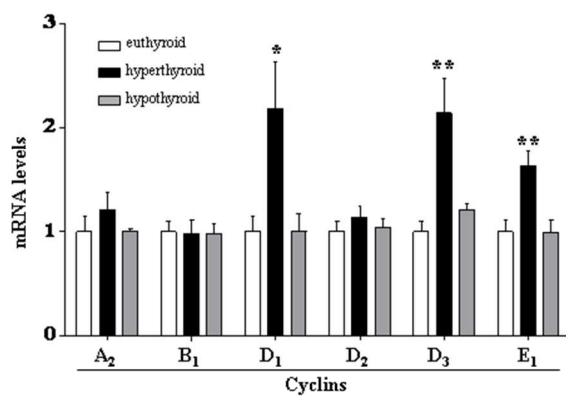190x254mm (96 x 96 DPI)
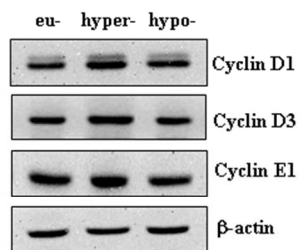
Figure 4
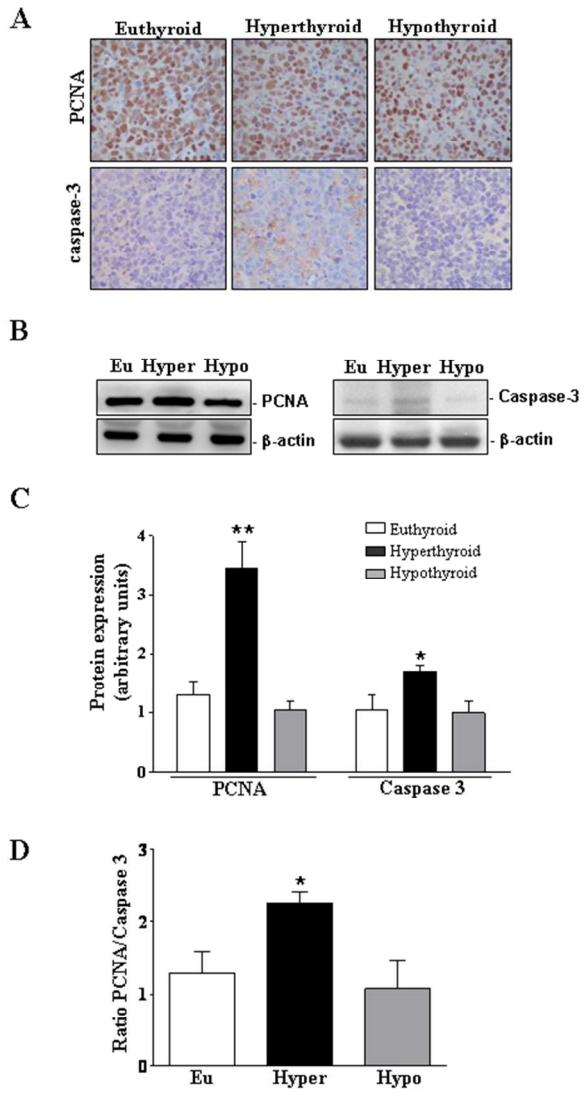
Effects of thyroid status on the cellular proliferation and apoptosis of the tumor tissue
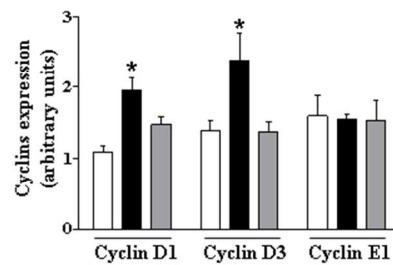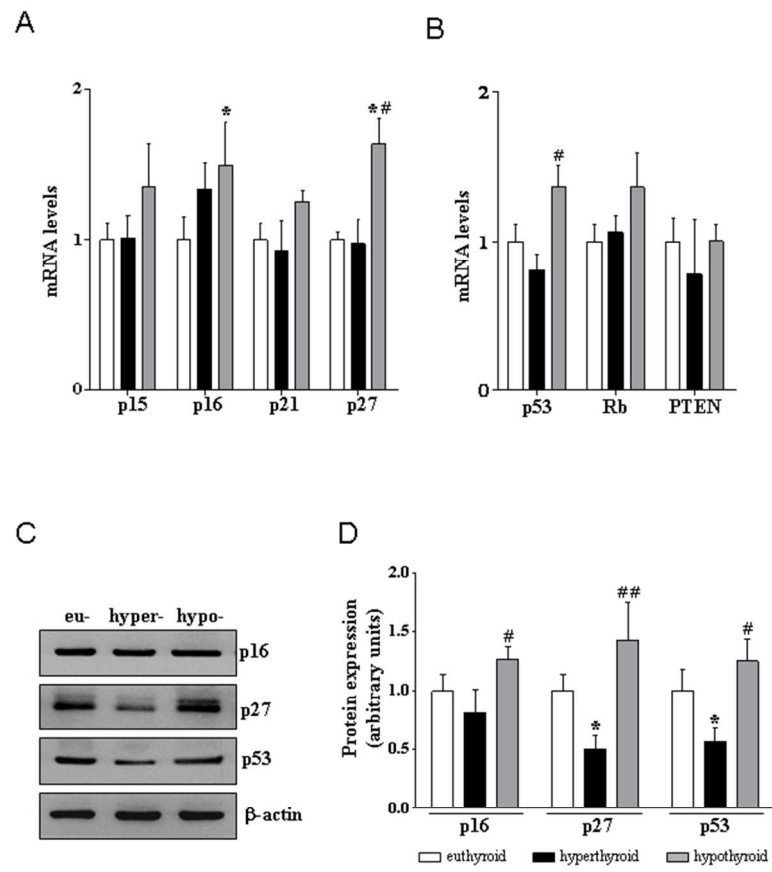190x254mm (96 x 96 DPI)

Figure 5

A

B

C

Effects of thyroid status on the expression of cell cycle regulatory proteins
190x254mm (96 x 96 DPI)

Figure 6

Effect of thyroid status on cyclin inhibitors and tumor suppressor proteins
190x254mm (96 x 96 DPI)

Table 1: Primer sequences used for real time RT-PCR analysis.

Gene	Primer Sequences	Tm (°C)
Cyclin A2	5'-GGCCAGCTGAGCTTAAAGAAAC-3' 5'-CGGGTAAAGAGACAGCTGCAT-3'	58.3 58.1
Cyclin B1	5'-AGGGTCGTGAAGTGACTGGAAACA-3' 5'-CTTGGGCACACAACTGTTCTGCAT-3'	60.2 60.3
Cyclin D1	5'-CCAAAACCATTCCATTTCAAAG-3' 5'-CCAACACACACCAGCAACACT-3'	57.2 58.1
Cyclin D2	5'-ACTTCAAGTTTGCCATGTACCCGC-3' 5'-TTCAGCAGCAGAGCTTCGATTTGC-3'	60.1 60.2
Cyclin D3	5'-TGCGTGCAAAAGGAGATCAA-3' 5'-TCACACACCTCCAGCATCCA-3'	59.0 59.7
Cyclin E1	5'-TGCTACTTGACCCACTGGACTCT-3' 5'-TGGCGTGGCCTCCTTAAC-3'	58.9 58.2
p15/INK4B	5'-TGGGAAACCTGGAGAGTAGATGA-3' 5'-GAATCCCCACACATGACAGTACA-3'	58.7 58.3
p16/INK4A	5'-CTCAACTACGGTGCAGATTCGA-3' 5'-CACCGGGCGGGAGAA-3'	59.0 58.5
p21/Cip1	5'-TGTGGCTCCCTCCCTGTCT-3' 5'-GCAGGGTGCTGTCCCTTCT-3'	59.2 58.8
p27/Kip1	5'-CCTGGCTCTGCTCCATTTGA-3' 5'-ACGGATGGAGCGCAAAAC-3'	59.9 58.2
p53	5'-GCATCCCGTCCCCATCA-3' 5'-GGATTGTGTCTCAGCCCTGAA-3'	59.8 58.7
Rb	5'-GGTCTGCCAACACCCACAA-3' 5'-GATGTCCCAAATGATTCACCAA-3'	58.9 58.2
PTEN	5'-GGTTCTTGGAAAACGGTGCTTAT-3' 5'-TGAAACCTCCCATGTGCTGAT-3'	59.4 59.0
β₂ microglobulin	5'-GCTATCCAGAAAACCCCTCAA-3' 5'-CATGTCTCGATCCCAGTAGACGGT-3'	62.0 62.0

The primers were designed using the mouse cDNA sequences in the UniGene database, following the criteria established by the Primer Express software (Applied Biosystems, California, USA).

1